LOAN DOCUMENT

PHOTOGRAPH THIS SHEET

DTIC ACCESSION NUMBER

LEVEL

INVENTORY

Effect of Trajectory Shaping on Observability of NTW Interceptor In-Flight Alignment Errors

DOCUMENT IDENTIFICATION

1999

DISTRIBUTION STATEMENT A
Approved for Public Release
Distribution Unlimited

DISTRIBUTION STATEMENT

ACCESSION FOR
NTIS GRA&I
DTIC TRAC
UNANNOUNCED
JUSTIFICATION

BY
DISTRIBUTION/
AVAILABILITY CODES

DISTRIBUTION	AVAILABILITY AND/OR SPECIAL	
A-1		

DISTRIBUTION STAMP

DATE ACCESSIONED

DATE RETURNED

20000814 199

DATE RECEIVED IN DTIC

REGISTERED OR CERTIFIED NUMBER

PHOTOGRAPH THIS SHEET AND RETURN TO DTIC-FDAC

HANDLE WITH CARE

DTIC FORM 70A JUN 90

DOCUMENT PROCESSING SHEET

PREVIOUS EDITIONS MAY BE USED UNTIL STOCK IS EXHAUSTED.

LOAN DOCUMENT

DTIC QUALITY INSPECTED 4

EFFECT OF TRAJECTORY SHAPING ON OBSERVABILITY OF NTW INTERCEPTOR IN-FLIGHT ALIGNMENT ERRORS

Ernest J. Ohlmeyer*
Naval Surface Warfare Center
Dahlgren, VA

Thomas R. Pepitone†
Aerospace Technology, Inc.
Dahlgren, VA

David B. Hanger**
Naval Surface Warfare Center
Dahlgren, VA

ABSTRACT

Navigation system and in-flight alignment requirements for a Navy Theater Wide (NTW) tactical ballistic missile interceptor are discussed. The missile navigation system is externally aided with both GPS and radar data for dynamic alignment and calibration of the missile's navigation system during flight. System alignment errors arise from missile in-canister initialization, ship navigation errors, and ship radar face misalignments. Reduction of these errors during flight is critical so that the rather small field-of-view of the Kinetic Warhead (KW) seeker can acquire and divert successfully to the target. The extent to which attitude errors are removed depends on the accuracy of the measurements, the kinematic activity in the trajectory, and the degree of observability associated with the state error dynamics. An observability metric is developed and used to quantify a measure of error state observability and evaluate the potential benefits afforded by intentional trajectory shaping. Several trajectory shaping techniques including nominal and aggressive launch azimuth biases, vertical plane shaping, and sinusoidal lateral plane maneuvers are investigated. Handover alignment accuracy is determined throughout the tactical engagement envelope and compared to NTW system requirements. The study also quantifies the value added of combining GPS and radar aiding data for in-flight alignment versus the use of radar alone.

INTRODUCTION

Many offensive and defensive missile systems require accurate alignment of the onboard inertial navigation system (INS) in order to achieve a high probability of kill against their intended targets. For systems in which time is not critical, this alignment process can be performed prior to launch by utilizing navigation data from the launch platform, and calibrating the missile's INS to this reference. However, for systems that require rapid reaction time, significant pre-launch delays for alignment are not tolerable. In this case, the launch platform can provide only a single initialization, and the alignment process must be performed after launch during the missile's flight.

This in-flight alignment utilizes acceleration and angular rate data from an inertial measurement unit (IMU), together with data (such as GPS or radar) provided by external sensors during flight. Differences between the INS state estimates and the external data are used by a Kalman navigation filter to generated error corrections that remove, over time, the effects of initial alignment errors and other types of navigation errors. For flights of sufficient duration, these errors can be brought to tolerable levels before commencement of the missile's terminal guidance phase, where accurate alignment is essential.

The extent to which in-flight alignment can reduce potentially large initial attitude errors and INS position and velocity errors will depend on several factors. These include the accuracy of the measurements processed by the INS (e.g., IMU, GPS and radar data), as well as the amount of kinematic activity in the missile's trajectory. Very accurate in-flight alignment usually requires a sufficient *richness* in the accelerations and angular rates experienced by the missile during flight.

In developing operational scenarios and trajectories that enhance error state observability, it is highly desirable to have a measure of effectiveness that quantifies the degree of observability of certain navigation system errors along specific trajectories. Recently, a new performance measure for in-flight observability has been developed and analyzed to assess its effectiveness. Termed the *Attitude Dilution of Precision* (ADOP), this measure was proposed in [1], later extended to include additional error states and state process noise in [2], and successfully used to predict the in-flight alignment performance of a Tactical Ballistic Missile Defense (TBMD) interceptor missile.

The TBMD example in [3] clearly illustrates how a missile's terminal effectiveness can depend critically on accurate in-flight alignment. The ship-launched interceptor is a multi-stage missile that incorporates a kinetic kill vehicle as the final, homing stage. During initialization by the ship, the missile's INS inherits a large initial alignment error in its body-to-earth direction cosine matrix. During flight, this can give rise to errors in pointing the terminal seeker for target acquisition, as well as guidance errors induced by rotating the inertially referenced acceleration commands into the misaligned body frame.

Since the terminal infrared seeker has a rather narrow field-of-view, uncompensated alignment errors can have a devastating effect on seeker acquisition, and may necessitate a large volume seeker scan, which can delay and even jeopardize acquisition. These difficulties can be overcome by implementing in-flight alignment wherein the external GPS or radar measurements allow the missile's INS to correct the alignment error during the midcourse flyout phase.

*Associate Fellow, AIAA
† Senior Member, AIAA
** Member, AIAA

The ADOP metric is developed to include the dominant system error sources and is then used as a measure of effectiveness in designing trajectories with enhanced error state observability. Using the system characteristics of a conceptual TBMD interceptor, several trajectory shaping schemes are proposed and analyzed for their in-flight alignment performance. Finally, conclusions from this preliminary study are presented.

ATTITUDE DILUTION OF PRECISION

ADOP is based on the navigation error propagation equations written in the Earth Centered, Earth Fixed (ECEF) frame [4-5]. Define the 15-element state vector as

$$\underline{X} = \left[\underline{\delta R}^T \underline{\delta V}^T \underline{\phi}^T \underline{\varepsilon}^T \underline{\delta L}^T\right]^T \tag{1}$$

where, $\underline{\delta R}^E, \underline{\delta V}^E$ are the INS position and velocity errors, and $\underline{\phi}^E$ is the body-to-ECEF attitude error. Superscripts $(\,)^E$ and $(\,)^R$ denote the ECEF and radar frames, respectively.

Also included are errors associated with use of the ship's tracking radar to provide in-flight updates to the missile's INS as shown in Figure 1. The radar measurements are contaminated by misalignment errors in the phased array radar faces, and in the ship's inertial navigator. These errors are embodied in the radar bias state $\underline{\varepsilon}^R$ which is coordinatized in the radar frame. The $\underline{\varepsilon}^R$ state is defined as the error in the transformation between the radar face and ECEF coordinate frames. The components of the $\underline{\varepsilon}$ error are the radar face misalignment (error between radar and ship deck) and the ship navigator's attitude error (error between ship deck and ECEF frame).

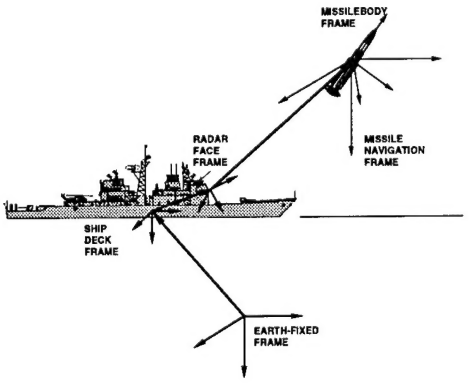

Figure 1. TBMD Coordinate Frames

An additional error introduced by the ship is a position bias error $\underline{\delta L}^E$, which is expressed in the ECEF frame. The INS calculates the missile position relative to the earth center. The radar measures the missile position with respect to the ship. Thus, in forming the measurement residual for the navigation Kalman filter, an error is introduced representing the ship navigator's positional error with respect to the ECEF frame.

It is also desirable to incorporate state process noise into the formulation. With the introduction of the new error states and process noise, the INS error dynamics can be written:

$$\begin{bmatrix} \underline{\delta\dot{R}}^E \\ \underline{\delta\dot{V}}^E \\ \underline{\dot{\phi}}^E \\ \underline{\dot{\varepsilon}}^R \\ \underline{\delta\dot{L}}^E \end{bmatrix} = \begin{bmatrix} 0 & I & 0 & 0 & 0 \\ A_{21} & A_{22} & A_{23} & 0 & 0 \\ 0 & 0 & A_{33} & 0 & 0 \\ 0 & 0 & 0 & 0 & 0 \\ 0 & 0 & 0 & 0 & 0 \end{bmatrix} \begin{bmatrix} \underline{\delta R}^E \\ \underline{\delta V}^E \\ \underline{\phi}^E \\ \underline{\varepsilon}^R \\ \underline{\delta L}^E \end{bmatrix} + \begin{bmatrix} \underline{w}_1 \\ \underline{w}_2 \\ \underline{w}_3 \\ \underline{w}_4 \\ \underline{w}_5 \end{bmatrix} \tag{2}$$

$$\begin{aligned} A_{21} &= G - \tilde{\Omega}^E \tilde{\Omega}^E \\ A_{22} &= -2\tilde{\Omega}^E \\ A_{23} &= \tilde{a}^E \\ A_{33} &= -\tilde{\Omega}^E \end{aligned} \tag{3}$$

where G is the gravity gradient matrix, $\tilde{\Omega}^E$ is the earth rate, and $\tilde{a}^E$ is the specific force, the latter two expressed as skew-symmetric matrices. Then Equation (2) may be written

$$\dot{\underline{X}} = A\underline{X} + \underline{w} \tag{4}$$

or, in discrete form, as

$$\underline{X}_k = \Phi(k, k-1)\underline{X}_{k-1} + \underline{w}_{k-1} \tag{5}$$

where $\underline{w}_k$ is a white noise sequence with covariance matrix Q_k. The state at time k can be related to the initial state by:

$$\underline{X}_k = \Phi(k,0)\underline{X}_0 + \underline{\alpha}_{k-1} \tag{6}$$

where

$$\underline{\alpha}_{k-1} = \underline{w}_{k-1} + \Phi(k,k-1)\underline{w}_{k-2} + \Phi(k,k-2)\underline{w}_{k-3} + \cdots + \Phi(k,2)\underline{w}_1 + \Phi(k,1)\underline{w}_0 \tag{7}$$

The measurement equation is

$$\underline{z}_k = h_k \underline{X}_k + \underline{v}_k \tag{8}$$

where $\underline{v}_k$ is measurement noise. In the case of GPS aiding, the observation matrix is:

$$h = \begin{bmatrix} I & 0 & 0 & 0 & 0 \\ 0 & I & 0 & 0 & 0 \end{bmatrix} \tag{9}$$

For radar aiding, the h matrix may be obtained as [3]:

$$h = \left[I \quad 0 \quad 0 \quad -\tilde{R}^E C_R^E \quad -I\right] \tag{10}$$

where $\underline{R}$ is missile range from the initial ship position, and $\tilde{R}$ represents a skew-symmetric matrix. The calculation of h for the radar case also requires C_R^E as a function of time. This implies that a ship motion time history must be specified. Substituting Equation (6) into Equation (8) gives

$$\underline{z}_k = h_k \Phi(k,0)\underline{X}_0 + \underline{u}_k \tag{11}$$

where

$$\underline{u}_k = h_k \underline{\alpha}_{k-1} + \underline{v}_k \tag{12}$$

is an augmented noise sequence, in which the components $\underline{\alpha}$ and $\underline{v}$ are uncorrelated. Then the terms at each k are stacked so that

$$\underline{Z} = \begin{bmatrix} \underline{z}_1 \\ \underline{z}_2 \\ \bullet \\ \bullet \\ \bullet \\ \underline{z}_N \end{bmatrix} \quad H = \begin{bmatrix} h_1\Phi(1,0) \\ h_2\Phi(2,0) \\ \bullet \\ \bullet \\ \bullet \\ h_N\Phi(N,0) \end{bmatrix} \quad \underline{U} = \begin{bmatrix} h_1\underline{\alpha}_0 + \underline{v}_1 \\ h_2\underline{\alpha}_1 + \underline{v}_2 \\ \bullet \\ \bullet \\ \bullet \\ h_N\underline{\alpha}_{N-1} + \underline{v}_N \end{bmatrix} \tag{13}$$

or

$$\underline{Z} = H\underline{X}_0 + \underline{U} \tag{14}$$

Now define the covariance matrices

$$\begin{aligned} V_k &= Cov(\underline{v}_k) \\ S_k &= Cov(\underline{\alpha}_k) \\ R_k &= Cov(\underline{u}_k) \end{aligned} \tag{15}$$

Since $\underline{\alpha}$ and $\underline{v}$ are uncorrelated, the covariance of $\underline{u}$ is given by

$$R_k = h_k S_{k-1} h_k^T + V_k \tag{16}$$

In computing R_k, it is convenient to use the following recursions for $\underline{\alpha}$ and S:

$$\underline{\alpha}_k = \underline{w}_k + \Phi(k+1,k)\underline{\alpha}_{k-1} \tag{17}$$

$$S_k = Q_k + \Phi(k+1,k)S_{k-1}\Phi(k+1,k)^T \tag{18}$$

Then

$$R = Cov(\underline{U}) = diag(R_1, R_2, \cdots, R_N) \tag{19}$$

Equations (14)-(19) describe a generalized least squares (LS) problem [6], where the goal is to estimate the vector $\underline{X}_0$, given the set of measurements $\underline{Z}$, corrupted by the noise $\underline{U}$.

The covariance of the LS estimation error is given by

$$P = [P_0^{-1} + H^T R^{-1} H]^{-1} = [P_0^{-1} + \sum_{k=1}^{N} H_k^T R_k^{-1} H_k]^{-1} \tag{20}$$

where k denotes the k^{th} measurement set. The initial body-to-ECEF attitude error $\underline{\phi}_0$ can be related to the initial state vector $\underline{X}_0$ by

$$\underline{\phi}_0^E = \begin{bmatrix} 0 & 0 & I & 0 & 0 \end{bmatrix} \underline{X}_0 = C_1 \underline{X}_0 \tag{21}$$

The vector $\underline{\psi}$ represents the error in the transformation from the radar frame to the missile body frame. Using the previous definitions for $\underline{\phi}$ (body to ECEF) and for $\underline{\varepsilon}$ (radar to ECEF), the error $\underline{\psi}$ may be written:

$$\underline{\psi}^E = \underline{\varepsilon}^E - \underline{\phi}^E = C_R^E \underline{\varepsilon}^R - \underline{\phi}^E \tag{22}$$

The initial value of $\underline{\psi}$ can be related to the initial state vector $\underline{X}_0$ by:

$$\underline{\psi}_0^E = \begin{bmatrix} 0 & 0 & -I & C_{R0}^E & 0 \end{bmatrix} \underline{X}_0 = C_2 \underline{X}_0 \tag{23}$$

The initial ship position bias state $\underline{\delta L}_0$ may be normalized by the radius of the earth to create an angular error $\underline{\theta}_0$. Then $\underline{\theta}_0$ expressed in the ECEF frame may be related to the initial state vector by:

$$\underline{\theta}_0^E = \begin{bmatrix} 0 & 0 & 0 & 0 & (1/R_E) \end{bmatrix} \underline{X}_0 = C_3 \underline{X}_0 \tag{24}$$

The covariances associated with these errors may be determined from

$$\begin{aligned} P_1 &= Cov(\underline{\phi}_0) = C_1 P C_1^T \\ P_2 &= Cov(\underline{\psi}_0) = C_2 P C_2^T \\ P_3 &= Cov(\underline{\theta}_0) = C_3 P C_3^T \end{aligned} \tag{25}$$

To calculate ADOP transformation matrices are found that diagonalize the P_1, P_2, and P_3 matrices. Then for each, the square root of the largest diagonal component is used to obtain ADOP for that metric. The goal is to find a matrix B such that

$$\overline{P}_1 = B P_1 B^T \tag{26}$$

is diagonal. To solve for B, one finds the eigenvalues λ_i of the matrix P_1. Then it can be shown [7]

$$\overline{P}_1 = \begin{bmatrix} \lambda_1 & 0 & 0 \\ 0 & \lambda_2 & 0 \\ 0 & 0 & \lambda_3 \end{bmatrix} \tag{27}$$

Physically, this corresponds to finding a coordinate transformation which makes the x,y,z attitude error components uncorrelated. The distribution of errors in the new system is then an ellipsoid with the largest error component lying along the principal axis. This largest error component is equal to the square root of the maximum eigenvalue of the P_1 matrix. The three scalar components of a vector ADOP may then be calculated from

$$\underline{ADOP} = 3000 \begin{bmatrix} [\lambda_{MAX}(P_1)]^{1/2} \\ [\lambda_{MAX}(P_2)]^{1/2} \\ [\lambda_{MAX}(P_3)]^{1/2} \end{bmatrix} \tag{28}$$

In Equation (28), the square root of the maximum eigenvalue is multiplied by 1000 to convert from radians to milliradians, and by 3 to form a 3σ estimate. In lieu of eigenvalue decomposition, an approximation for ADOP may be obtained by taking the square root of the sum of the three diagonal components of each P_i matrix.

APPLICATIONS TO NAVY THEATER WIDE MISSILE DEFENSE

Use of the ADOP metric will now be illustrated using a Theater Missile Defense scenario. In this example, a ship-launched missile is used to defend against tactical ballistic missiles (TBMs) targeted for friendly land areas. The interceptor missile is intended to engage the TBM during the exoatmospheric portion of its flight prior to re-entry. To accomplish this, the conceptual interceptor consists of four stages as shown in Figure 2. These include a first stage booster, a second stage dual thrust rocket motor, a third stage dual pulse motor, and a fourth stage Kinetic Warhead (KW) for hit-to-kill destruction of the TBM.

Employment of the defensive missile is closely tied to the shipboard weapon control system. The ship's radar initially detects the target and develops a fire control solution. After the missile is launched, the ship uplinks acceleration commands (during 2nd Stage) or missile and target state data (during 3rd Stage) to enable the interceptor to close the collision triangle. At the end of 3rd Stage, the KW is released, acquires the target and maneuvers to intercept using divert propulsion. Figure 2 also illustrates the main events in the engagement sequence.

Essential to the success of the mission is the process of in-flight alignment performed on the missile. The missile utilizes in-flight measurements from GPS satellites [8-9] and from the ship's track radar [3] to update its INS. In particular, alignment errors arising from launch canister initialization, ship navigation errors and radar face misalignments must be reduced to very small values to allow the KW's narrow field of view to acquire the target.

The degree to which large initial alignment errors can be reduced to satisfactory levels depends strongly on the quality of the GPS and radar updates, and on the amount of thrusting the missile performs during its midcourse guidance phase. Missile accelerations improve the observability of the INS attitude errors and radar alignment errors compared to periods of non-thrusting ballistic flight.

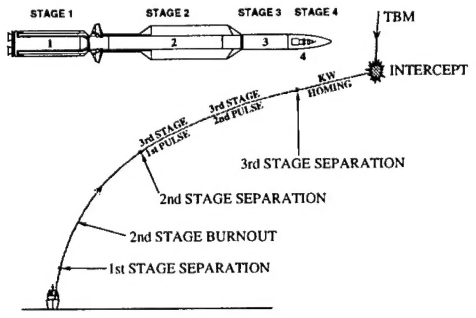

Figure 2. TBMD Missile - System Overview

The ADOP metric can be used to quantify the amount of attitude error observability as a function of the missile's flight profile and acceleration history. The various ADOP metrics described earlier can be associated with particular attitude errors critical to the missile's in-flight alignment. For example, the $\underline{\phi}$ error describes how accurately the KW's body orientation is known relative to an earth-fixed coordinate frame, in which celestial objects are specified. Since the KW must recognize known objects and distinguish them from the true target, this error must be minimized for successful target acquisition.

The $\underline{\psi}$ error is important when the missile uses only radar data for in-flight alignment, without GPS. In this case, the missile guidance is performed in a relative coordinate frame containing the radar and missile. Since the radar is the sensing device and the missile's strapdown INS is body referenced, the transformation between radar and body must be accurately known. The error in this transformation is represented by the attitude error $\underline{\psi}$. Any errors in the projection of missile thrust into the radar sensing frame will introduce an equivalent heading error into the midcourse guidance, which will contribute a guidance error at handover to the KW.

In the following sections, ADOP is used to quantify the attitude error observability and assess the impact of several trajectory shaping strategies with the intent of improving error state observability and hence in-flight alignment accuracy.

For selected cases, the ADOP alignment predictions were compared to alignment error calculations from a detailed INS/GPS/Radar Monte Carlo navigation simulation illustrated in Figure 3, and described in [10-11]. The navigation model included detailed modeling of the GPS satellites and GPS receiver errors, the ship's track radar and associated errors, the missile's IMU errors, and the INS and Kalman navigation filter processing used to blend the GPS and radar measurements with the INS navigation solution. Representative sets of missile and ship system errors were assumed for selected TBMD engagement scenarios.

A comparative summary of alignment performance predictions using both ADOP and the detailed Monte Carlo navigation simulation, for four tactical trajectories spanning the engagement envelope is shown in Table 1. The results illustrate that ADOP is a useful and computationally efficient metric for providing a lower bound on missile attitude errors during in-flight alignment.

Table 1. Comparison of ADOP Alignment Predictions & Monte Carlo Simulation Results

	$\underline{\phi}$ Alignment Error @ KW Ejection (mrad)			
Tactical Case	Radar Only		Radar & GPS	
	ADOP	NAVSIM	ADOP	NAVSIM
2	12.9	15.7	2.7	4.2
3	21.4	22.5	3.2	3.8
6	19.2	21.8	3.7	5.8
11	16.3	18.2	3.0	4.2

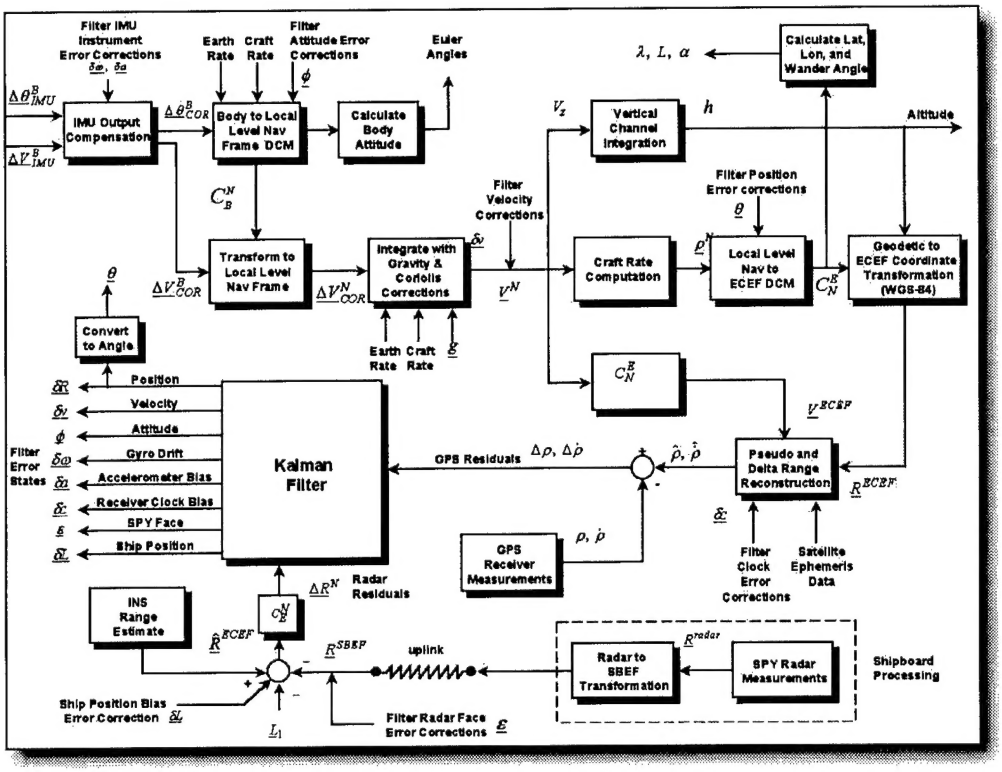

Figure 3. GPS/SPY/INS Integrated System

TRAJECTORY SHAPING ANALYSIS

The ADOP metric may be used to quantify the amount of attitude error observability as a function of the missile's flight profile and acceleration history. The ADOP technique can also be used to generate *observability maps* of the error metrics over a full engagement envelope or *battlespace*. The resulting contour plot of ADOP versus ground range and altitude can be used to compare the effectiveness of different sensors such as GPS or radar. In addition, the observability maps graphically illustrate regions in the engagement envelope where poor observability causes problems for in-flight alignment. The regions of poor observability have led to re-evaluation and redesign of trajectories through modified trajectory shaping methods in an attempt to improve observability.

In this analysis, a family of guided flight profiles was generated for intercept points over a complete engagement envelope using the baseline guidance methodology and system parameters outlined in reference [12]. The baseline guidance methodology utilizes limited trajectory shaping in the vertical plane. For each intercept point in this ground range-altitude grid, the ADOP metric was computed along the missile trajectory and recorded at the desired evaluation time (i.e., at the KW release point). The values of the metric associated with each intercept point were then used to generate contour plots or ADOP maps over the battlespace. Figure 4 displays the resulting contour maps of the ADOP metric at the KW release point for the baseline trajectories. The white dots indicate the set of feasible intercept points. The legend in Figure 4 defines the gray shading scheme for the ADOP contours in all the ADOP maps given throughout this paper.

These ADOP maps clearly illustrate the improvement in the attitude error observability resulting from the use of GPS aiding. The radar plus GPS aiding map indicates that the ADOP metric satisfies the attitude error requirement of 5 mrad (3σ) for in-flight alignment over the majority of the battlespace. Conversely, the radar-only aiding map shows that the ADOP metric fails to meet the attitude error requirement over the entire battlespace, with the central region having the worst observability.

Since the ADOP metric is a function of the flight profile and the acceleration history, the application of different trajectory shaping methods could possibly modify the observability of the attitude error. To improve the attitude error observability, particularly for the case of radar-only aiding, the following five trajectory shaping methods were considered:

- Nominal offset angle of the first stage commanded bearing angle
- Aggressive offset angle of the first stage commanded bearing angle
- Nominal second stage horizontal plane weave
- Aggressive second stage horizontal plane weave
- Increase in the first stage commanded flight path angle (VLEG) from 70 degrees to 80 degrees

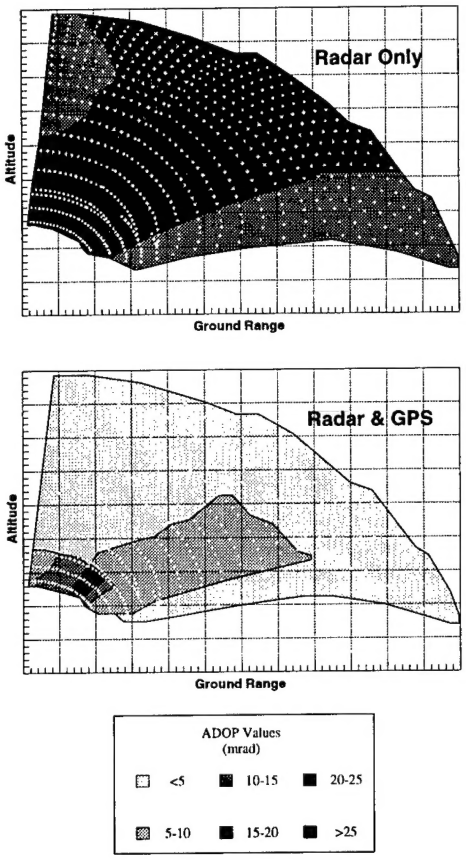

Figure 4. ADOP Contour Maps for the Baseline Trajectories

The first four methods add trajectory shaping to the horizontal plane. The final method modifies the existing vertical plane trajectory shaping. For each of the trajectory shaping methods, a family of trajectories to intercept points covering the entire engagement envelope was generated. Then the ADOP metric was computed along the trajectories, and the value at the KW release point for each trajectory was used to create new observability maps. The ADOP maps for each trajectory shaping method were compared to the baseline maps to determine the effects of trajectory shaping on the attitude error observability.

The first two trajectory shaping methods add a horizontal offset angle to the commanded launch bearing angle. The commanded bearing angle is computed at launch and aligns the interceptor trajectory with the vertical plane containing the intercept point. The offset angle puts the interceptor trajectory during first stage guidance along a bearing angle outside of the vertical intercept plane. The offset angle is removed during second stage when the guidance produces horizontal plane trajectory shaping that realigns the trajectory parallel to the launch vertical intercept plane.

The magnitude of the offset angle is computed as a linear function of the cosine of the angle between the launch line-of-sight to the intercept point and the vector along the first stage commanded flight path (VLEG). This function relates the size of the offset angle and the amount of trajectory shaping to the location of the intercept point within the envelope. Figure 5 shows the relationship of the nominal offset angle to the ground range and altitude coordinates of the intercept point. The maximum nominal offset angle is 25 degrees for intercepts along the vector defined by a 70 degree angle in the vertical plane. The offset angle decreases to zero as the vertical plane angle to the intercept point decreases to zero. To perform the aggressive offset angle trajectory shaping, the offset angle is set to twice the nominal offset angle.

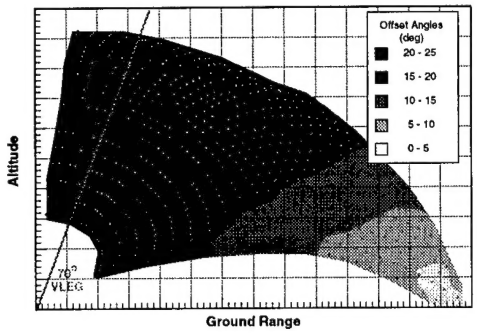

Figure 5. Contours of the Nominal Offset Angle across the Engagement Envelope

To ensure that the offset trajectory returns to being parallel to the launch vertical intercept plane, the horizontal plane guidance gain is made a multiple of two of the vertical plane guidance gain. The horizontal trajectory shaping resulting from either the nominal or aggressive offset angles does not significantly effect the interceptor's flight profile in the vertical plane or the intercept velocity. Figure 6 illustrates a sample baseline interceptor trajectory and the corresponding nominal and aggressive offset angle trajectories. Figure 7 contains the velocity profiles for these same trajectories.

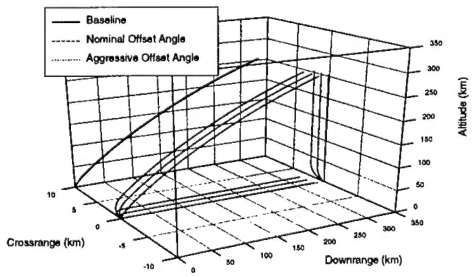

Figure 6. Trajectory Comparisons for Bearing Offset Angles

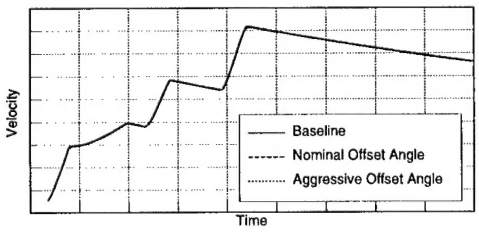

Figure 7. Velocity Profile Comparisons for Bearing Offset Angles

The ADOP maps for offset angle shaping were generated for the cases of radar-only aiding and radar plus GPS aiding of the in-flight alignment. The resulting

contour maps for the nominal offset angle are given in Figure 8. The ADOP maps for the aggressive offset angle are shown in Figure 9.

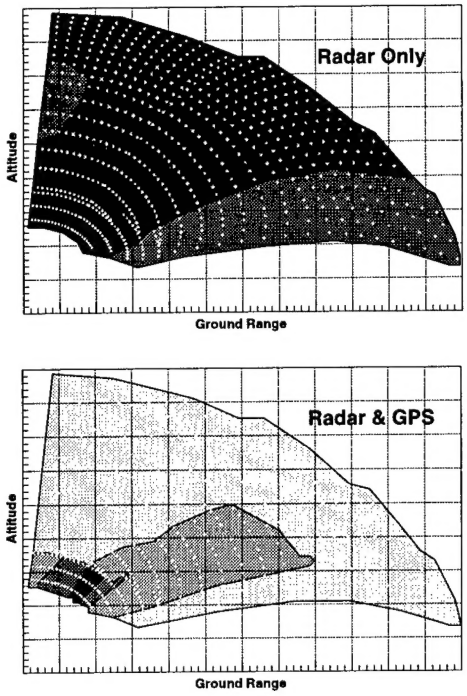

Figure 8. ADOP Contour Maps for the Nominal Offset Angle Trajectories

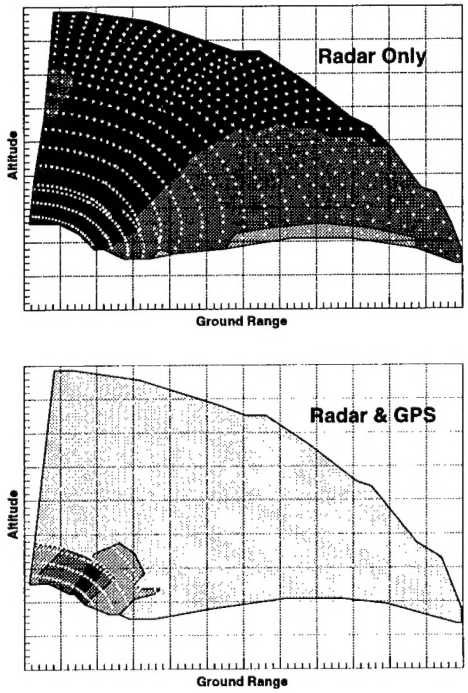

Figure 9. ADOP Contour Maps for the Aggressive Offset Angle Trajectories

Figure 8 indicates that the nominal offset angle trajectory shaping provides only minimal improvements to the attitude error observability. For in-flight alignment with radar-only aiding, the ADOP metric continues to violate the 5 mrad (3σ) attitude error requirement across the entire battlespace. The shaping causes only minor improvements in the central region of the battlespace. The radar and GPS aiding map for the nominal offset angle shaping is also largely unchanged from the baseline case.

ADOP maps with the aggressive offset angle trajectory shaping show greater improvement in the observability of the attitude error. The radar and GPS aiding contour map of Figure 9 shows an increase in the favorable region of the battlespace. However, for the radar-only aiding case of Figure 9, the improvement is marginal, and the radar-only aiding still fails to achieve the required alignment accuracy.

The next shaping method considered is horizontal plane weaving. The goal of the nominal and aggressive weave trajectory shaping is to add maneuvers to the horizontal plane to improve the attitude error observability. These methods apply a sinusoidal weave to the commanded bearing angle during the second stage guidance. The weave is initiated at the beginning of the second stage with an amplitude of 10 degrees and a period of 5 seconds. The weave amplitude decays linearly with altitude to zero throughout the second stage. As in the offset angle trajectory shaping methods, the nominal weave uses a horizontal plane guidance gain that is a multiple of 2 of the vertical plane guidance gain. The aggressive weave uses a horizontal plane gain that is a multiple of 6 of the vertical. As shown in Figure 10, the larger guidance gain for the aggressive weave results in greater responsiveness to the commanded bearing angle.

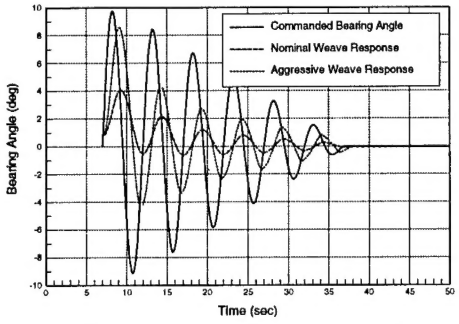

Figure 10. Bearing Angle Response for the Horizontal Plane Weave

Both the nominal and aggressive horizontal plane weave maneuvers have only a minor impact on the vertical plane flight profile of the interceptor (less than a 5% loss of range and intercept velocity). Figures 11 and 12 contain trajectory and velocity comparisons for a sample trajectory.

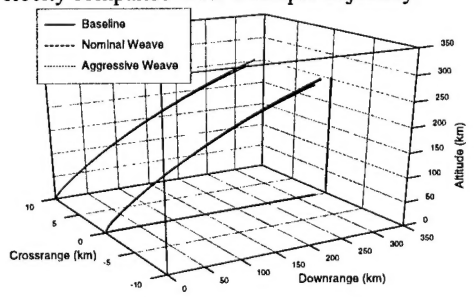

Figure 11. Trajectory Comparisons for Horizontal Plane Weaves

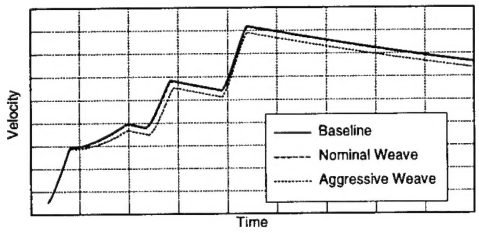

Figure 12. Velocity Profile Comparisons for Horizontal Plane Weaves

Using both nominal and aggressive horizontal plane weave maneuvers, ADOP maps were generated for both radar-only aiding and simultaneous radar and GPS aiding. The resulting ADOP contour maps for the nominal weave are given in Figure 13, and results for the aggressive weave are shown in Figure 14.

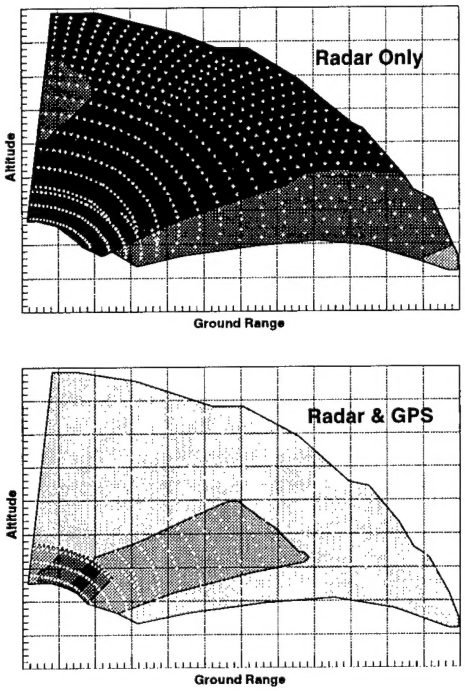

Figure 13. ADOP Contour Maps for the Nominal Horizontal Plane Weave Trajectories

The ADOP maps in Figures 13 and 14 indicate no improvement in attitude error observability over the baseline trajectories. For both nominal and aggressive weaves, the radar-only ADOP maps fail to satisfy the in-flight alignment requirement and show little change over the baseline maps except at the higher altitudes. In some cases, observability for the high altitude intercepts is reduced rather than improved with the horizontal plane weaves. For the nominal weave, the radar and GPS aiding ADOP map of Figure 13 is essentially unchanged from the baseline map. The radar and GPS aiding map of Figure 14 for aggressive weave shows an increase in the acceptable in-flight alignment region.

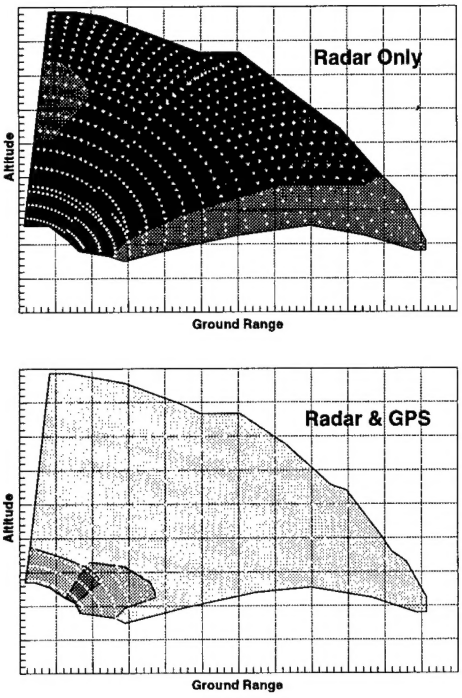

Figure 14. ADOP Contour Maps for the Aggressive Horizontal Plane Weave Trajectories

The final trajectory shaping method intended to improve attitude error observability modifies the commanded vertical flight path angle of the first stage, or VLEG. The baseline VLEG is specified as 70 degrees. The modified trajectory shaping increased the VLEG to 80 degrees. While increasing VLEG provides no trajectory shaping to the horizontal plane, the trajectory shaping in the vertical plane is increased for a majority of the intercepts in the battlespace. By increasing this angle to 80 degrees, a larger pull down maneuver is required during the second stage to reach any intercept points below a vertical plane angle of 70 degrees. Intercepts above the 80 degree angle require a smaller pull up maneuver.

Although increasing VLEG typically increases the vertical plane acceleration, the trajectory profile and velocity history are not significantly changed. Figure 15 illustrates the minor differences between the baseline 70 degree and the 80 degree VLEG trajectories. The velocity profile for these two trajectories is given in Figure 16. Note for these cases that the vertical plane angle of the line to the intercept point is well below the 80 degree vector.

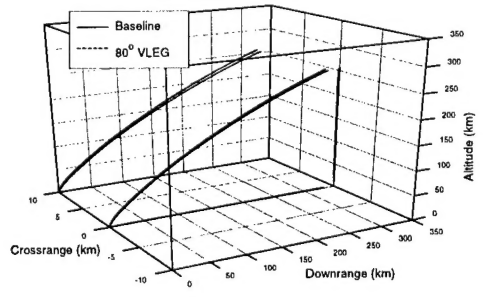

Figure 15. 70° and 80° VLEG Trajectory Comparison

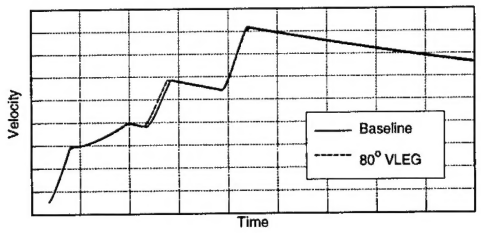

Figure 16. 70° and 80° VLEG Velocity Profile Comparison

With an 80 degree VLEG for the first stage, new ADOP maps were generated for both radar-only aiding and radar plus GPS aiding. The resulting maps are given in Figure 17.

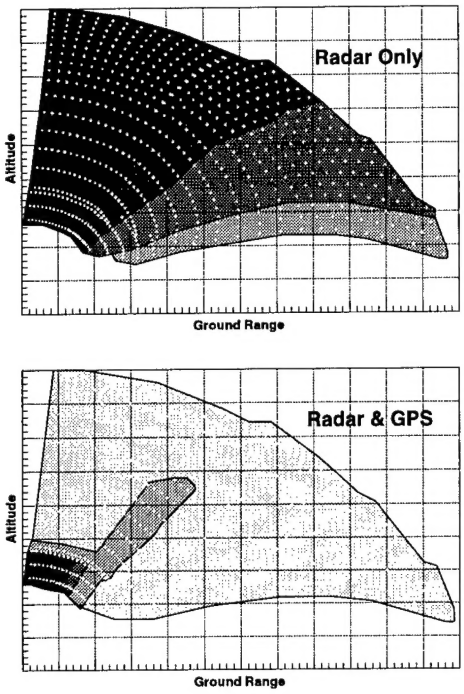

Figure 17. ADOP Contour Maps for the 80° VLEG

Again, the ADOP map for radar-only aiding violates the in-flight alignment requirement across the entire battlespace. As anticipated, the ADOP contours for both aiding methods are shifted towards the larger vertical plane angles. This shift in the ADOP contours results in improved observability at the lower angles (i.e. below 70 degrees) and reduced observability at the higher angles. The shift generally corresponds to the increased vertical plane maneuvers required during the second stage for the 80 degree VLEG.

CONCLUSIONS

The Attitude Dilution of Precision (ADOP) metric was defined and used to evaluate attitude error observability along typical TBMD interceptor trajectories. Flyout trajectories which had displayed poor attitude error observability in previous studies, were modified with the inclusion of several candidate trajectory shaping techniques for the purpose of enhancing error state observability and thus improving in-flight alignment accuracy. Five techniques for second stage trajectory shaping were investigated to improve the in-flight alignment across the battlespace, particularly for the case of radar-only aiding. In comparison to the baseline trajectories for radar-only and for radar plus GPS aiding, the trajectory shaping methods showed only marginal improvements in the in-flight alignment. For all of the trajectory shaping methods, the radar aided in-flight alignment failed to satisfy attitude error requirements across the battlespace. For both the baseline case and the trajectory shaping cases, the radar plus GPS aiding provided significant improvements in observability and satisfied attitude error requirements over the vast majority of the battlespace. Use of GPS thus provides a significant performance advantage over radar-only aiding for in-flight alignment of NTW missiles.

ACKNOWLEDGEMENT

The authors wish to acknowledge the contributions of the following individuals at NSWCDD: Thomas Hymer, who provided the six degree-of-freedom missile trajectories, and Craig Phillips and Mark Jones who designed the guidance algorithms used in the TBMD example.

REFERENCES

[1] Johnson, Carl, *A Metric for In-flight Alignment, "ADOP", Attitude Dilution of Precision*, unpublished briefing material, Dec 16, 1998.

[2] Ohlmeyer, E. J., unpublished working papers, Feb 3 and Oct 18, 1999.

[3] Ohlmeyer, E. J. and Pepitone, T. R., *In-Flight Removal of TBMD System Alignment Errors Using GPS and Radar Measurements*, 6th Annual AIAA/BMDO Technology Readiness Conference, San Diego, CA, August 1997.

[4] Regan, F. J., "Strapdown Systems, Part II, Algorithms," Naval Surface Warfare Center Technical Note TN 81-409, Silver Spring, MD, November, 1981. See also: Dynamics of Atmospheric Re-Entry, AIAA Education Series, Washington, DC, 1993, Chapter 14.

[5] Ohlmeyer, E. J. and Pepitone, T. R., *Assessment of Integrated GPS/INS for the EX-171 Extended Range Guided Munition*, AIAA Guidance, Navigation and Control Conference, Boston, MA, August 1998.

[6] Sorenson, H., Parameter Estimation, Marcel Dekker, Inc, New York, NY, 1980, Chapter 2.

[7] Strang, G., Linear Algebra and Its Applications, HBJ, San Diego, 1988, 3rd Edition, pp. 254-256.

[8] Kaplan, Elliott D., Ed., Understanding GPS, Principles and Applications, Artech House, Norwood, MA, 1996.

[9] Parkinson, Bradford W., Spilker, James J., Axelrad, Penina and Enge, Per, Global Positioning System: Theory and Applications, Vols. I and II, American Institute of Aeronautics and Astronautics, Washington, DC, 1995.

[10] Ohlmeyer, E. J., Pepitone, T. R., Miller, B. L., Malyevac, D. S., Bibel, J. E., Evans, A. G., "System Modeling and Analysis of GPS/INS for Extended Range Guided Munitions," TR 96/159, Dahlgren Division, Naval Surface Warfare Center, Dahlgren, VA, August, 1996.

[11] Ohlmeyer, E. J., Pepitone, T. R., Miller, B. L., Malyevac, D. S., Bibel, J. E., Evans, A. G., *GPS-Aided Navigation System Requirements for Smart Munitions and*

Guided Missiles, Proceedings of AIAA Guidance Navigation, and Control Conference, New Orleans, LA, 1997, pp.954-968.

[12] Phillips, C. A. and Jones, M. A., *Tactical Considerations for SM-3 Second and Third Stage Guidance,* AIAA Missile Sciences Conference, Nov 1998.